Refractive Index-Modulated LSPR Sensing in 20–120 nm Gold and Silver Nanoparticles: A Simulation Study

ECS Sensors Plus, 2023 **2** 043402

Refractive Index-Modulated LSPR Sensing in 20–120 nm Gold and Silver Nanoparticles: A Simulation Study

Zoe Bradley,[1] David Cunningham,[1] and Nikhil Bhalla[1,2,z]

[1]*Nanotechnology and Integrated Bioengineering Centre (NIBEC), School of Engineering, Ulster University, Belfast BT15 1AP, United Kingdom*
[2]*Healthcare Technology Hub, School of Engineering, Ulster University, Belfast, BT15 1AP, United Kingdom*

Localized surface plasmon resonance (LSPR) based sensing has been a simple and cost-effective way to measure local refractive index changes. LSPR materials exhibit fascinating properties that have significant implications for various bio/chemical sensing applications. In many of these applications, the focus has traditionally been on analyzing the intensity of the reflected or transmitted signals in terms of the refractive index of the surrounding medium. However, limited simulation work is conducted on investigating the refractive index sensitivity of LSPR materials. Within this context, here we simulate the refractive index sensing properties of spherical gold (Au) and silver (Ag) nanoparticles ranging from 20–120 nm diameter within 1.0 to 1.50 refractive index units (RIU). After analyzing the peak optical efficiency and peak wavelength, we report the sensing performance of these materials in terms of sensitivity, linearity and material efficiency, which we refer to as the figure of merit (FOM). Overall, our observations have revealed greatest FOM values for the smallest sized nanoparticles, a FOM of 6.6 for 20 nm AuNPs and 11.9 for 20 nm AgNPs with refractive index of 1.

 [DOI: 10.1149/2754-2726/ad08d8]

Manuscript submitted September 3, 2023; revised manuscript received October 17, 2023. Published November 16, 2023.

Refractive index (RI) based Localized Surface Plasmon Resonance (LSPR) biosensing is a powerful label-free tool in the field of biosensing research.[1–3] This technique utilizes the changes in RI caused by the binding of molecules to the surface of noble metallic nanostructures, which in turn affects the LSPR peak wavelength and total absorbance of light by the nanostructures.[4] Fundamentally, when light interacts with the LSPR nanoparticles, it creates a collective oscillation of the conduction electrons on the surface of the nanoparticles.[5] This oscillation is highly sensitive to changes in the RI of the surrounding medium. In bio/chemical sensing applications, a layer of molecules, such as antibodies, DNA probes or even cells, when immobilized on the surface of the metallic nanoparticles results in the change of local RI around the nanoparticles.[6] Further, changes in the local RI around the nanoparticles are resulted when a target molecule binds to these molecules, which causes a shift in the LSPR wavelength peak and total absorbance of light nanostructures.[7] By monitoring this shift in the LSPR peak wavelength or absorbance, the binding of the target molecule can be detected, calibrated, and quantified.

The sensitivity of LSPR biosensing is highly dependent on the size, shape, and composition of the metallic nanoparticles used.[8,9] In general, smaller nanoparticles exhibit higher sensitivity to changes in RI, while larger nanoparticles exhibit lower sensitivity but higher signal-to-noise ratios to changes in RI.[10,11] The shape of the nanoparticles can also affect sensitivity, with complex anisotropic particles, for example, nanorods, nanostars or nanotriangles exhibiting higher sensitivity compared to their isotropic counterparts, which are typically spherical nanoparticles. This is due to anisotropic nanoparticles having different dimensions along their three axes, which results in a more complex electron oscillation pattern compared to isotropic nanoparticles, which have the same properties and dimensions in all directions.[12,13] Additionally, the electric field is more concentrated at the tips of anisotropic particles, which can result in a stronger LSPR signal and therefore higher sensitivity.[14] However, isotropic nanoparticles have a more uniform electron oscillation pattern, which makes them more stable by being less sensitive to changes in the environment conditions, such as changes in pH or temperature.[15]

Gold nanoparticles (AuNPs) and silver nanoparticles (AgNPs), both spherical in shape are popular nanostructures used within LSPR biosensing due to their unique optical properties, including high extinction coefficients and strong plasmonic resonance peaks in the visible and near-infrared regions.[16,17] For quality LSPR biosensors, nanoparticles must have good optical properties which are displayed by a narrow absorption peak and particles should display a good adhesion to analytes of interest.[18] Both AuNPs and AgNPs are biocompatible and can be functionalized with a wide variety of analytes, including proteins, DNA, bacteria, and viruses.[19–22] Several works in the literature are published demonstrating numerous applications in the fields of biomedical research, clinical diagnostics, and environmental monitoring using AuNPs and AgNPs with LSPR sensors. A recent study by Ryu and Ha used LSPR to investigate how the thickness of a silver coating on silver-coated gold nanorods (Ag@AuNRs) affects sensor sensitivity with respect to changes in RI. Thicker coatings of silver around the nanorods showed higher sensitivity levels which demonstrates the impact of silver in enhancing LSPR sensitivity.[23] Another study by Kim et al used a seed mediated growth method to immobilize optical fibers with AuNPs to enhance LSPR RI sensitivity and overall stability.[24]

Within this work, we simulate the effects of RI based LSPR biosensing on AuNPs and AgNPs from sizes 20–120 nm diameter, that are spherical in shape. Nanoparticles in the size range of 20–120 nm diameter have been selected for this simulation as they are mostly used for LSPR-based sensing due to their unique plasmonic properties and high surface area-to-volume ratio, which leads to enhanced sensitivity compared to bulk materials.[25,26] RI of 1.00, 1.33, 1.35, 1.40, 1.45 and 1.50 have been used for the simulation to help researchers understand the behaviour of AuNPs and AgNPs in different RI environments to improve nanoparticle size selection for future work on the development of bio/chemical sensors. The RI is an important parameter in LSPR-based sensing to determine the sensitivity, selectivity, and effectiveness of the sensor in detecting and quantifying changes in the local environment, such as the binding of molecules to the surface of nanoparticles.[27] There are some works in the literature which have investigated the optical efficiency and scattering of gold nanoparticles of different sizes and shapes in air and water.[28–31] However, to the best of our knowledge, there is no work which has comprehensively investigated the optical efficiencies and scattering of Au and Ag spherical nanoparticles of sizes from 20–120 nm. This includes investigation of its RI sensitivities in media of RI 1.00–1.50, and elucidation of theoretical FOM (by simulations) of each size of AuNPs and AgNPs. Therefore,

[z]E-mail: n.bhalla@ulster.ac.uk

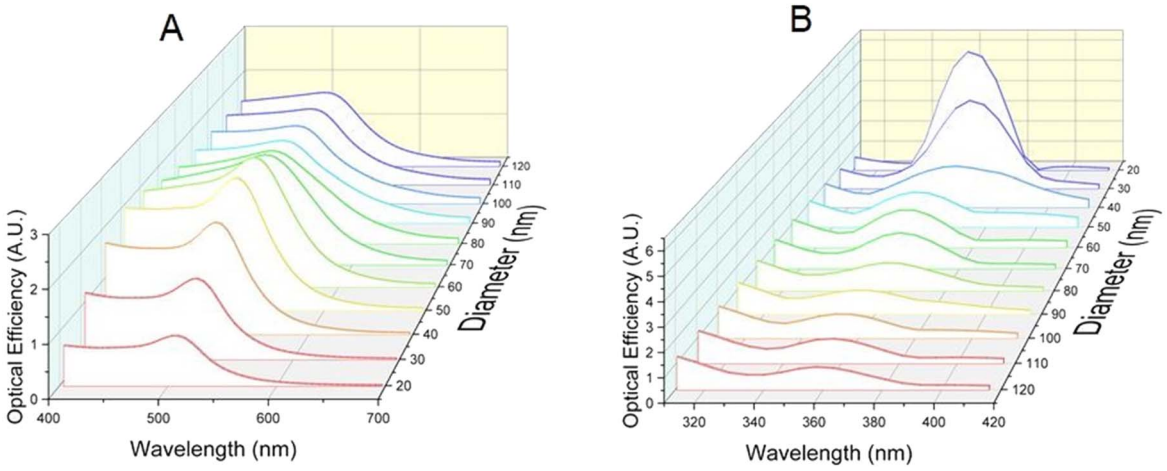

Figure 1. LSPR spectra in air (R.I. = 1): LSPR spectra showing the optical efficiency (O.E.) of (A) AuNPs and (B) AgNPs. The size of the nanoparticles ranges from 20–120 nm diameter in periods of 10 nm.

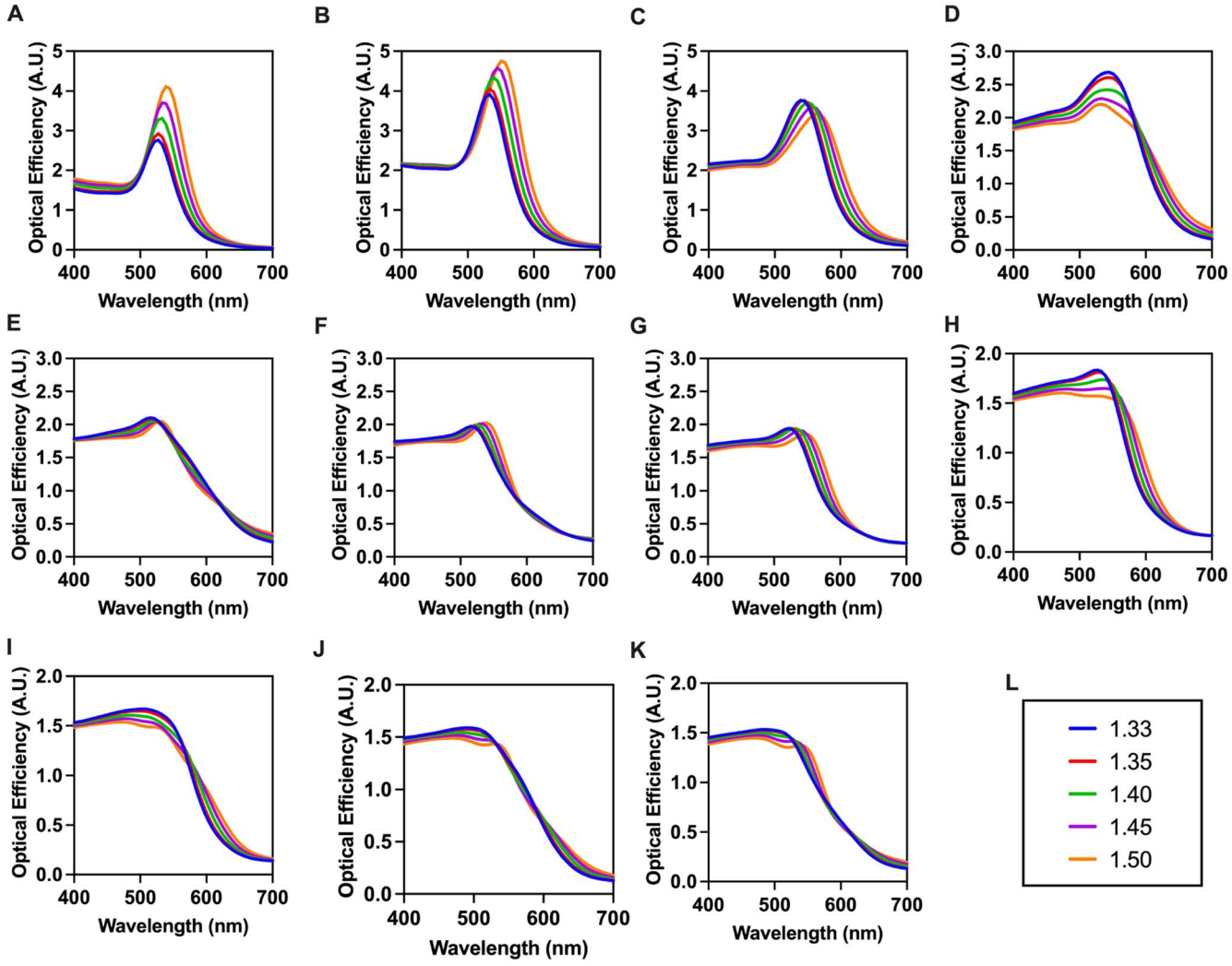

Figure 2. LSPR properties of AuNPs with change in the refractive index of AuNPs: LSPR spectra of (A)–(K) 20–120 nm respectively of different RI (1.33, 1.35, 1.40, 1.45 and 1.50). (L) shows the legends corresponding to colors of graphs in (A)–(K).

our manuscript offers a distinct contribution by presenting a comprehensive simulation study on a range of AuNPs and AgNPs. This unique approach will enable researchers to select the most suitable nanoparticle size for specific sensing applications. As a result, our report serves as a reliable and valuable guide for a wide range of researchers working with Ag and Au nanoparticles.

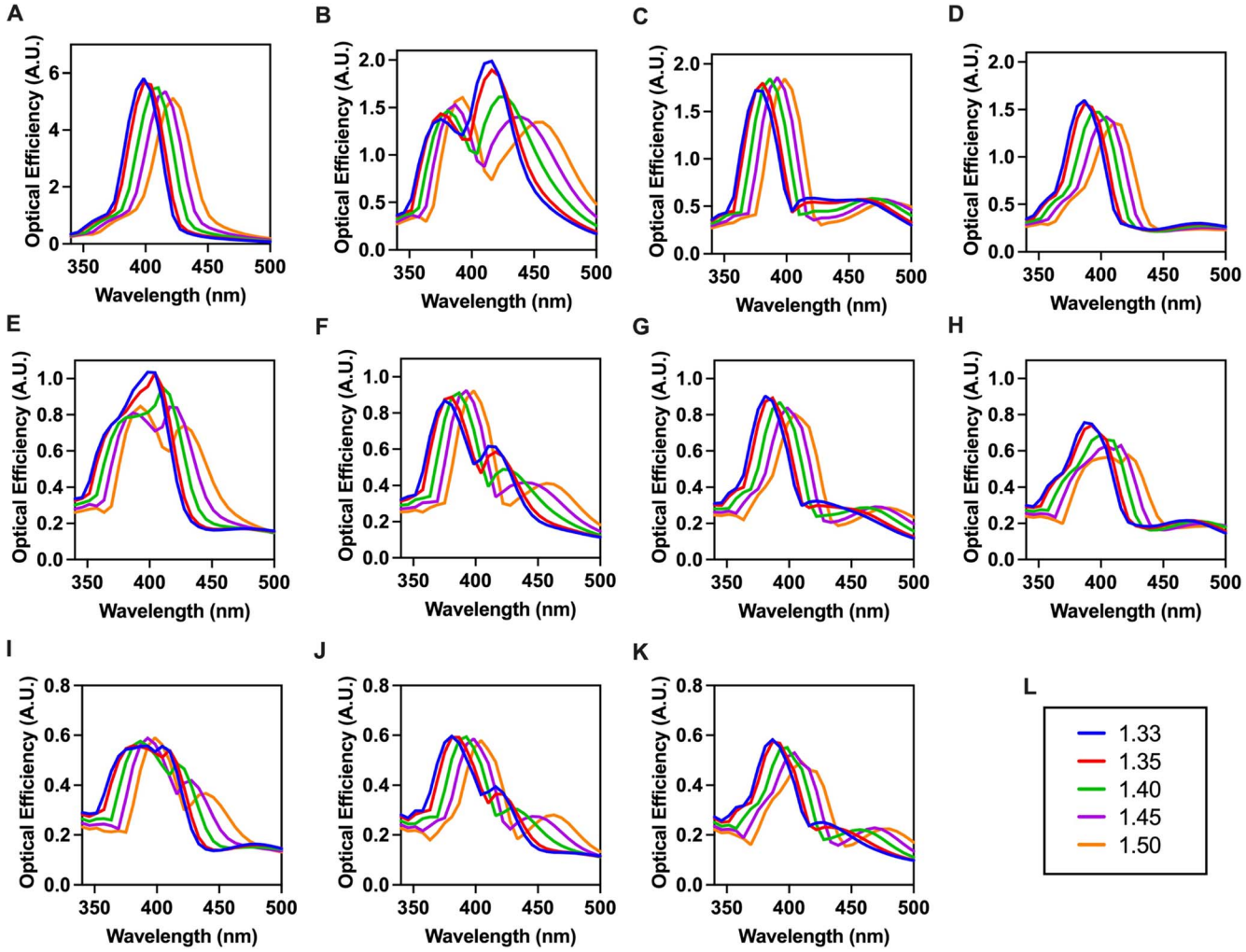

Figure 3. LSPR properties of AgNPs with change in the refractive index of AgNPs: LSPR spectra of (A)–(K) 20–120 nm respectively of different RI (1.33, 1.35, 1.40, 1.45 and 1.50). (L) shows the legends corresponding to colors of graphs in (A)–(K).

Simulations

All simulations are performed using Nanosphere Optics Lab (NOL) from nanohub platform. This tool is produced by researchers at Northewestern University. NOL calculates the absorption, scattering, and extinction spectra of spherical nanoparticles using the Mie theory. The in-built features of NOL also enable calculations for a range of particle sizes for both Au and Ag. Using NOL, we simulated the nanoparticle optical efficiency (OE) which is the scattering cross-section to extinction ratio. The OE has been calculated by using the Eq. 1 from the Mie theory:[32]

$$OE = \frac{Csca}{Cext} - \frac{Csca}{Csca + Cabs} \quad [1]$$

These cross-section parameters can be determined by expanding the internal and scattered fields into a series of partial waves, which are modeled by vector harmonics within NOL. The original calculations can be found in C.F. Bohren and D.R. Huffman's book "Absorption and Scattering of Light by Small Particles."[33]

Results and Discussion

Figures 1A and 1B display the LSPR spectrum of gold nanoparticles (AuNPs) and silver nanoparticles (AgNPs) in air (RI = 1.00) respectively. First, it is important to understand the behaviour and trends that are presented by AuNPs and AgNPs simulation in air (RI = 1.00) before studying the effects which the changing RI can have on particle OE. Figure 1A shows that the size 60 nm AuNPs has the narrowest spectra with an optical efficiency (OE) of 2.6 and a peak wavelength of 515 nm.

As AuNPs size increases there is a shift in the peak wavelength and after the size 60 nm, there is a broadening in the peak. More features associated with the direction of shifts are explained in detail later. On the other hand, Fig. 1B shows that the AgNPs of size 20 nm has the narrowest spectra with an OE of 5.8 and peak wavelength of 357 nm. A clear trend is seen with AgNPs behaviour at RI = 1.00 i.e., as the particle size increases the peak OE decreases, and the peak broadens which leads to a reduction in optical efficiency.

Figures 2A–2K displays the simulation results of 20–120 nm AuNPs with different RI of 1.33, 1.35, 1.40, 1.45 and 1.50. A broadening in the absorption peak, red shift in the peak wavelength and a decrease in peak OE is seen as AuNPs increase in size. Within individual AuNPs sizes a common trend shows that as the RI increases, the peak OE also increases with a red shift in the peak wavelength. For example, in Fig. 2A, the 20 nm AuNPs in a RI media of 1.33 has a peak OE of 2.8 and a peak wavelength of 527 nm which increases to a peak OE of 4.1 and peak wavelength of 538 nm at RI 1.50.

Similarly, Figs. 3A–3K displays the simulation results of 20–120 nm AgNPs with different RI of 1.33, 1.35, 1.40, 1.45 and 1.50. Like AuNPs, AgNPs display a red shift in the peak wavelength as the particle size and RI increases. However, the peak OE

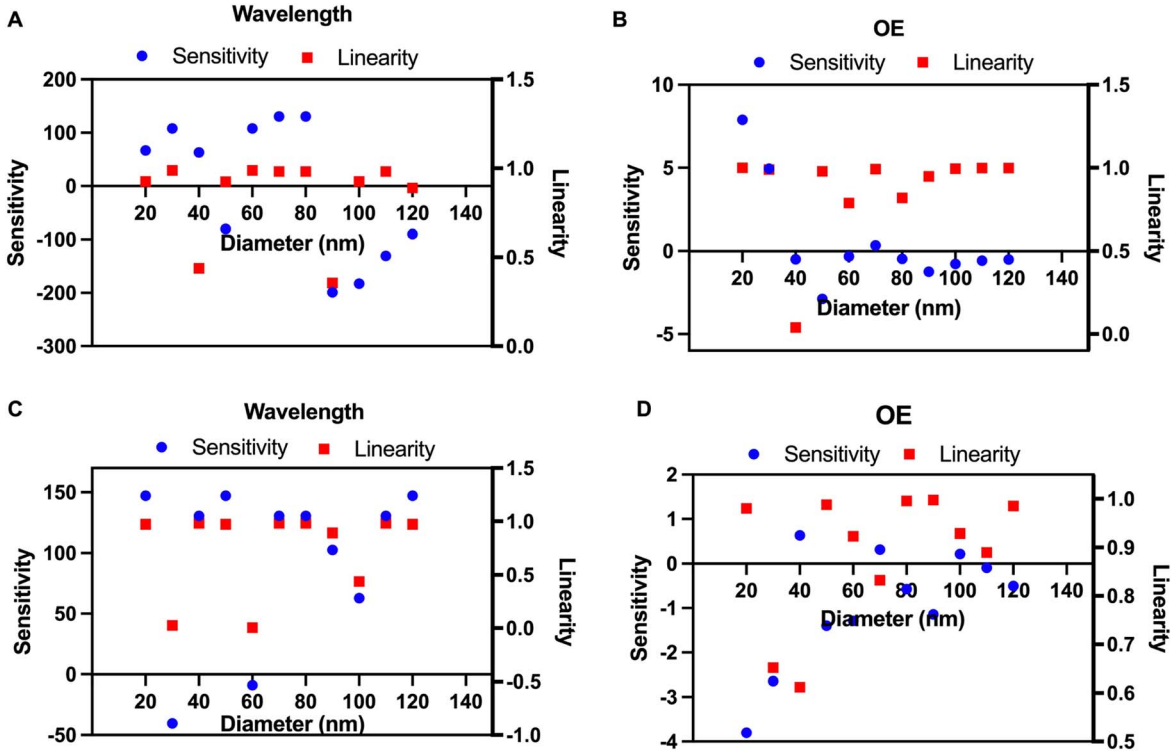

Figure 4. LSPR sensitivity and linearity analysis: (A) AuNPs peak wavelength. (B) AuNPs peak OE (C) AgNPs peak wavelength (D) AgNPs peak OE.

decreases as the RI increases, for example within Fig. 3A, 20 nm AgNPs in RI media of 1.33 has a peak OE of 5.8 and a peak wavelength of 398 nm which decreases to a peak OE of 5.1 and peak wavelength of 421 nm at RI 1.50.

To compare sensing performance of AuNPs and AgNPs of different diameter in different RI, sensitivity and linearity analysis from peak wavelength and peak OE are displayed in Figs. 4A–4D and figure of Merit (FOM) results are shown in Figs. 5A–5D. High values for both sensitivity and linearity regarding both peak wavelength and peak OE indicate excellent LSPR performance. From Fig. 4A, AuNPs peak OE indicates that regarding peak wavelength, size 60–80 nm AuNPs offer optimal performance while size 90 nm AuNPs performing poorly (comparatively to other sizes). However, regarding sensitivity and linearity results from peak OE of AuNPs, as seen in Fig. 4B, size 20 nm AuNPs offer the best sensing performance with 40 nm AuNPs performing the worst. Figure 4C indicates optimum sensitivity and linearity from 20 and 80 nm AgNPs and the poorest performance from 30 nm AgNPs regarding peak wavelength. Peak OE also shows poor performance from 30 nm AgNPs whilst 20 nm AgNPs has the worst sensitivity.

FOM is a quantitative measurement used to assess LSPR performance and efficiency. In our research, it serves as a benchmark for evaluating and comparing different nanoparticle diameters across different RI. In general, a higher FOM indicates better sensor performance.[34] FOM is determined by first calculating RI sensitivity (RIS), which is the ratio between the shift in plasmon resonance wavelength ($\Delta\lambda$LSPR) and the variation in the RI of the surrounding medium (Δn),[35] see Eq. 2:

$$RIS = \frac{\Delta\lambda\text{LSPR}}{\Delta n} \quad [2]$$

The RI sensitivity measurement cannot act as a standalone measurement for sensor performance, but it is used in determining FOM which is the ratio of the RIS to the full width at half resonance height (Full Width at Half Maximum (FWHM)), see Eq. 3:

$$FOM = \frac{RIS}{FWHM} \quad [3]$$

Figure 5A shows the FOM for each RI studied for each particle diameter between 20–120 nm. Overall, as the AuNPs diameter increases, the FOM decreases with RI 1.50 giving the best FOM result and RI 1.33 showing the lowest FOM result, indicating a AuNP of 20 nm diameter in RI 1.50 giving overall the best performance. This trend is also seen in Fig. 5B with 20 nm AuNPs having the highest FOM. A similar trend is seen in Fig. 5C and D with the 20 nm AgNPs having the largest FOM and then FOM starts to increase when RI is varied from 1.33 to 1.50.

Conclusions

This simulation shows the OE of spherical Au and Ag nanoparticles 20–120 nm diameter within different RIUs for LSPR-based sensing. With regards to AuNPs, our results show that smaller particles with higher RIU offer the greatest sensitivity, linearity and FOM. As AuNPs diameter increases there is a broadening of the peak, a redshift in the peak wavelength and a decrease in OE. A similar trend is also seen with AgNPs as the particle diameter and RI increase, there is a peak wavelength red shift, but a decline in peak OE as RI increases. Sensitivity and linearity results vary regarding peak wavelength and peak OE and therefore a more in-depth FOM analysis was carried out to better understand LSPR performance. High FOM values indicate excellent LSPR-based sensing performance with a trend across both Au and Ag nanoparticles showing that the smallest diameter particle size with the highest RI of 1.50 offers the best biosensor performance.

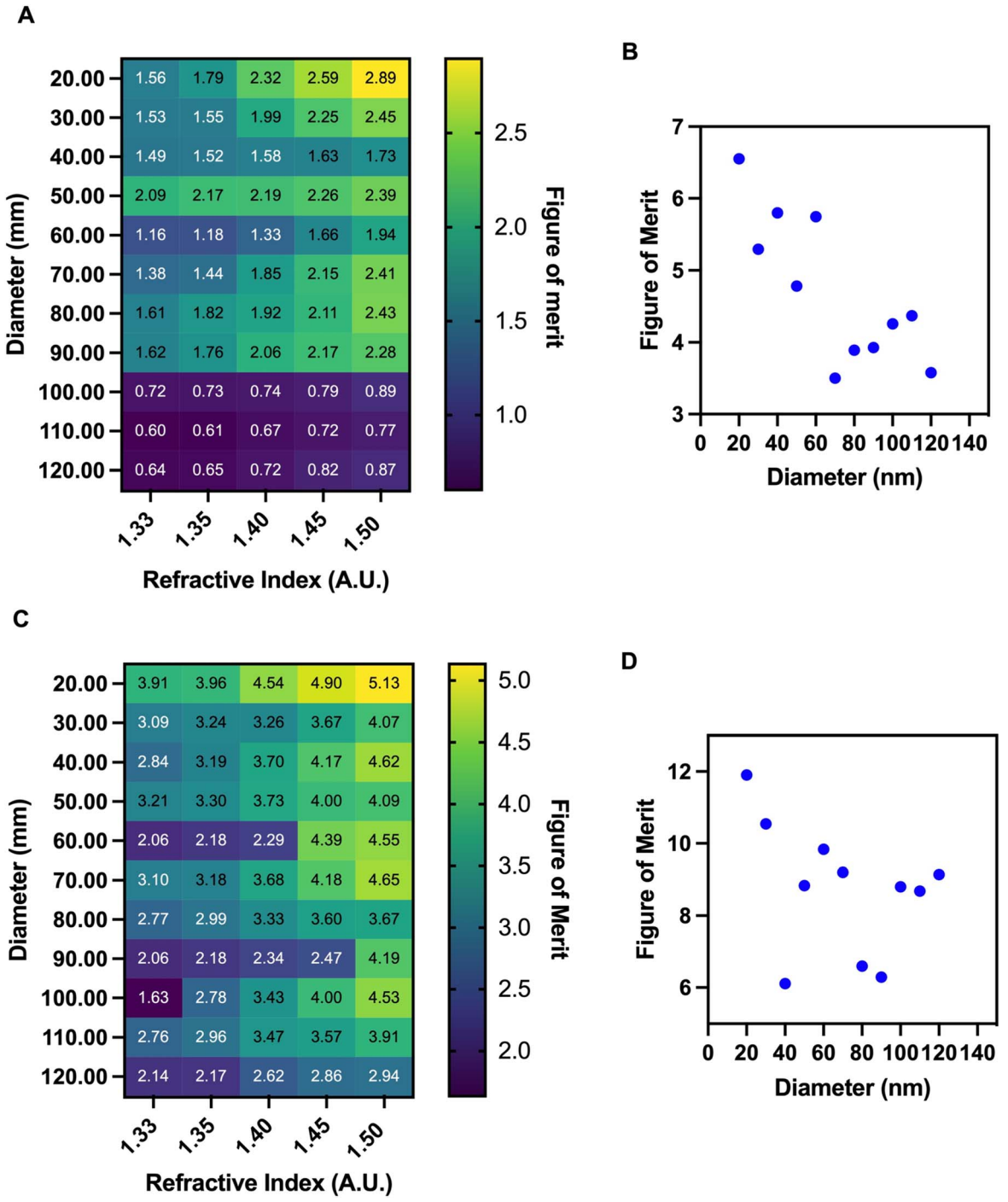

Figure 5. Figure of merit (FOM) analysis: (A) AuNPs in different RI (B) AuNPs in air (C) AgNPs in different RI (D) AgNPs in air.

ORCID

Zoe Bradley https://orcid.org/0000-0002-5561-315X
Nikhil Bhalla https://orcid.org/0000-0002-4720-3679

References

1. N. Bhalla, P. K. Sharma, and S. Chakrabarti, *ACS Omega*, **7**, 27664 (2022).
2. N. A. Curras, *ECS Sensors Plus*, **2**, 010001 (2023).
3. N. Bhalla, A. F. Payam, A. Morelli, P. K. Sharma, R. Johnson, A. Thomson, P. Jolly, and F. Canfarotta, *Sensors Actuators B*, **365**, 131906 (2022).
4. Y. Xu, P. Bai, X. Zhou, Y. Akimov, C. E. Png, L. K. Ang, W. Knoll, and L. Wu, *Adv. Opt. Mater.*, **7**, 1801433 (2019).
5. M. D'Acunto, P. Cioni, E. Gabellieri, and G. Presciuttini, *Nanotechnology*, **32**, 192001 (2021).
6. S. Kaushal, S. S. Nanda, S. Samal, and D. K. Yi, *ChemBioChem*, **21**, 576 (2020).
7. V. Khoshdel and M. Shokooh-Saremi, *Micro Nano Lett.*, **14**, 566 (2019).
8. M. Lu, H. Zhu, C. G. Bazuin, W. Peng, and J. F. Masson, *ACS Sens.*, **4**, 613 (2019).
9. V. Chugh, A. Basu, A. Kaushik, and A. K. Basu, *ECS Sensors Plus*, **2**, 015001 (2023).
10. H. Oh, A. Pyatenko, and M. Lee, *Appl. Surf. Sci.*, **542**, 148613 (2021).
11. J. L. Hammond, N. Bhalla, S. D. Rafiee, and P. Estrela, *Biosensors*, **4**, 172 (2014).
12. V. Pellas, D. Hu, Y. Mazouzi, Y. Mimoun, J. Blanchard, C. Guibert, M. Salmain, and S. Boujday, *Biosensors*, **10**, 146 (2020).
13. S. Wang, X. Huang, Q. An, R. Zhou, W. Xu, D. Xu, Q. Lin, and X. Cao, *Anal. Chim. Acta*, **1160**, 338380 (2021).
14. A. K. Pearce, T. R. Wilks, M. C. Arno, and R. K. O'Reilly, *Nature Reviews Chemistry*, **5**, 21 (2021).
15. Y. Ihm, D. H. Cho, D. Sung, D. Nam, C. Jung, T. Sato, S. Kim, J. Park, S. Kim, and M. Gallagher-Jones, *Nat. Commun.*, **10**, 2411 (2019).
16. M. Q. He, Y. L. Yu, and J. H. Wang, *Nano Today*, **35**, 101005 (2020).

17. A. Loiseau, V. Asila, G. Boitel-Aullen, M. Lam, M. Salmain, and S. Boujday, *Biosensors*, **9**, 78 (2019).
18. J. Ozhikandathil, S. Badilescu, and M. Packirisamy, *ECS Sensors Plus*, **1**, 023201 (2022).
19. L. Liu, A. Thakur, W. K. Li, G. Qiu, T. Yang, B. He, Y. Lee, and C. M. L. Wu, *Chem. Eng. J.*, **446**, 137383 (2022).
20. W. Ning, C. Zhang, Z. Tian, M. Wu, Z. Luo, S. Hu, H. Pan, and Y. Li, *Biosens. Bioelectron.*, **228**, 115175 (2023).
21. R. T. da Silva, M. V. Petri, E. Y. Valencia, P. H. Camargo, S. I. de Torresi, and B. Spira, *Photodiagn. Photodyn. Ther.*, **31**, 101908 (2020).
22. N. H. Moghadam, R. Najafi, A. Ghanbariasad, A. S. Dezfuli, and A. Jalali, *J. Biomol. Struct. Dyn.*, **41**, 1 (2023).
23. K. R. Ryu and J. W. Ha, *RSC Adv.*, **10**, 16827 (2020).
24. H. M. Kim, D. H. Jeong, H. Y. Lee, J. H. Park, and S. K. Lee, *Opt. Laser Technol.*, **114**, 171 (2019).
25. A. W. Zaibudeen and R. Bandyopadhyay, *Nanotechnology*, **34**, 295601 (2023).
26. R. Funari, K.-Y. Chu, and A. Q. Shen, *Biosens. Bioelectron.*, **169**, 112578 (2020).
27. P. Sui, A. Zhang, F. Pan, P. Chang, H. Pan, F. Liu, J. Wang, and C. Cao, *Opt. Laser Technol.*, **155**, 108427 (2022).
28. N. M. Saleh and A. A. Aziz, "Simulation of surface plasmon resonance on different size of a single gold nanoparticle." *J. Phys. Conf. Ser.*, **1083**, 012041 (2018).
29. A. R. Shafiqa, A. A. Aziz, and B. Mehrdel, "Nanoparticle optical properties: size dependence of a single gold spherical nanoparticle." *J. Phys. Conf. Ser.*, **1083**, 012040 (2018).
30. P. K. Jain, K. S. Lee, I. H. El-Sayed, and M. A. El-Sayed, *J. Phys. Chem. B*, **110**, 7238 (2006).
31. M. R. Rakhshani, *IEEE Sens. J.*, **22**, 4043 (2022).
32. N. L. Dmitruk, S. Z. Malynych, I. E. Moroz, and V. Y. Kurlyak, *Semiconductor physics quantum electronics and optoelectronics*, **13**, 369 (2010).
33. C. F. Bohren and D. R. Huffman, *Absorption and scattering of light by small particles* (Wiley-VCH, Germany) (1998).
34. K. Lodewijks, W. V. Roy, G. Borghs, L. Lagae, and P. V. Dorpe, *Nano Lett.*, **12**, 1655 (2012).
35. O. Haidar, A. Akjouj, and A. Mir, *Photonics and Nanostructures-Fundamentals and Applications*, **50**, 101016 (2022).